AAC Accepted Manuscript Posted Online 8 January 2018
Antimicrob. Agents Chemother. doi:10.1128/AAC.01909-17
Copyright © 2018 Nixon et al.
This is an open-access article distributed under the terms of the Creative Commons Attribution 4.0 International license.

Accepted Manuscript Posted Online
Antimicrobial Agents and Chemotherapy
AAC
Antimicrobial Agents and Chemotherapy

Downloaded from http://aac.asm.org/ on January 15, 2018 by guest

Pharmacodynamics of Flubendazole for Cryptococcal Meningoencephalitis: Repurposing and Reformulation of an Anti-Parasitic Agent for a Neglected Fungal Disease

Gemma. L. Nixon,[1,2] Laura McEntee,[2] Adam Johnson,[2] Nikki Farrington,[2] Sarah Whalley,[2] Joanne Livermore,[2] Cristien Natal,[2] Gina Washbourn,[1] Jaclyn Bibby,[1] Neil Berry,[1] Jodi Lestner,[2] Megan Truong,[3] Andrew Owen,[4] David Lalloo,[5] Ian Charles,[6] William Hope[2]*

[1]Department of Chemistry, University of Liverpool, Liverpool, United Kingdom

[2]Antimicrobial Pharmacodynamics and Therapeutics, Department of Molecular and Clinical Pharmacology, Institute of Translational Medicine, Liverpool, UK

[3]The ithree Institute, University of Technology Sydney, Sydney, Australia

[4]Department of Molecular and Clinical Pharmacology, H Block, Pembroke Place, Liverpool, UK

[5]Liverpool School of Tropical Medicine, Pembroke Place, Liverpool, UK

[6]The Quadram Institute Bioscience, Norwich Research Park, Norwich, NR47UA, UK

Corresponding Author

William Hope

Sherrington Building, Ashton Street, Liverpool, L69 3GE, United Kingdom

Phone +44 (0)151 794 5941

Accepted Manuscript Posted Online

Antimicrobial Agents and Chemotherapy

AAC

Antimicrobial Agents and Chemotherapy

Downloaded from http://aac.asm.org/ on January 15, 2018 by guest

19 *william.hope@liverpool.ac.uk

20

21 Keywords

22 *Cryptococcus neoformans*, cryptococcal meningoencephalitis, benzimidazole, flubendazole, β-

23 tubulin.

24

25 Acknowledgements

26 We thank Ana Alastruey-Izquierdo and Manual Cuenca Estrella (Mycology Reference Laboratory,

27 National Centre for Microbiology, Instituto de Salud Carlos III, Madrid, Spain) for kindly providing

28 *C. neoformans* clinical isolates; Benny Baeten, Ben Van Hove and Dr Petros Psathas (Janssen

29 Pharmaceutica) for providing the amorphous solid drug nanodispersion formulation of

30 flubendazole (batch BREC-1113-070); and, Peter Webborn and Stefan Kavanagh (Astrazeneca)

31 for their assistance with the *in vitro* DMPK data. Ian Charles acknowledges support from the

32 BBSRC. William Hope is supported by a National Institute of Health Research Clinician Scientist

33 Award (CS/08/08).

34 Potential Conflicts of Interest

35 William Hope holds or has recently held research grants with F2G, AiCuris, Astellas Pharma,

36 Spero Therapeutics, Matinas Biosciences, Antabio, Amplyx, Allecra, Auspherix and Pfizer. He

37 holds awards from the National Institutes of Health, Medical Research Council, National Institute

38 of Health Research, and the European Commission (FP7 and IMI). William Hope has received

Accepted Manuscript Posted Online

Antimicrobial Agents and Chemotherapy

AAC

Antimicrobial Agents and Chemotherapy

Downloaded from http://aac.asm.org/ on January 15, 2018 by guest

39 personal fees in his capacity as a consultant for F2G, Amplyx, Ausperix, Spero Therapeutics,
40 Gilead and Basilea. WH is Medical Guideline Director for the European Society of Clinical
41 Microbiology and Infectious Diseases, an Ordinary Council Member for the British Society of
42 Antimicrobial Chemotherapy. AO has received research funding from ViiV Healthcare, Merck,
43 AstraZeneca, and Janssen, and paid consultancy from Merck and ViiV Healthcare. Ian Charles is a
44 consultant for Auspherix.

45 Funding

46 This work was supported by Medical Research Council New Investigator grant to Dr Gemma
47 Nixon (MR/N023005/1) and the Institute of Food Research, Norwich, UK.

48

Accepted Manuscript Posted Online

Antimicrobial Agents and Chemotherapy

AAC

Antimicrobial Agents and Chemotherapy

Downloaded from http://aac.asm.org/ on January 15, 2018 by guest

ABSTRACT

Current therapeutic options for cryptococcal meningitis are limited by toxicity, global supply and emergence of resistance. There is an urgent need to develop additional antifungal agents that are fungicidal within the central nervous system and preferably orally bioavailable. The benzimidazoles have broad-spectrum anti-parasitic activity, but also have *in vitro* antifungal activity that includes *Cryptococcus neoformans*. Flubendazole (a benzimidazole) has been reformulated by Janssen Pharmaceutica as an amorphous solid drug nanodispersion to develop an orally bioavailable medicine for the treatment of neglected tropical diseases such as onchocerciasis. We investigated the *in vitro* activity, the structure-activity-relationships and both *in vitro* and *in vivo* pharmacodynamics of flubendazole for cryptococcal meningitis. Flubendazole has potent in vitro activity against *Cryptococcus neoformans* with a modal MIC of 0.125 mg/L using European Committee for Antimicrobial Susceptibility Testing (EUCAST) methodology. Computer models provided an insight into the residues responsible for the binding of flubendazole to cryptococcal ß-tubulin. Rapid fungicidal activity was evident in a hollow fiber infection model of cryptococcal meningitis. The solid drug nanodispersion was orally bioavailable in mice with higher drug exposure in the cerebrum. The maximal dose of flubendazole (12 mg/kg/day) orally resulted in a ~2 $\log_{10}$CFU/g reduction in fungal burden compared with vehicle-treated controls. Flubendazole was orally bioavailable in rabbits, but there were no quantifiable drug concentrations in the CSF or cerebrum and no antifungal activity was demonstrated in either CSF or cerebrum. These studies provide evidence for the further study and development of the benzimidazole scaffold for the treatment of cryptococcal meningitis.

Accepted Manuscript Posted Online

Antimicrobial Agents and Chemotherapy

AAC

Antimicrobial Agents and Chemotherapy

Downloaded from http://aac.asm.org/ on January 15, 2018 by guest

71

72 INTRODUCTION

73 Cryptococcal meningoencephalitis (herein meningitis) is a common and lethal disease in
74 immunosuppressed patients (1, 2). This disease is predominately associated with advanced HIV
75 infection and has the highest incidence in low to middle income countries (1). The number of
76 effective agents is despairingly small (3). All available induction and maintenance regimens are
77 constructed with three antifungal agents: amphotericin B (AmB), flucytosine (5FC) and
78 fluconazole (4). Each of these compounds has significant adverse effects that include infusional
79 toxicity (AmB), nephrotoxicity (AmB (5)), bone marrow suppression (AmB and 5FC (5, 6)) and
80 hepatotoxicity (fluconazole and 5FC (7)). Moreover, there are significant inherent limitations
81 that include fungistatic effects (fluconazole; (8)) and the potential emergence of drug resistance
82 (fluconazole and 5FC; (9–11)). Thus, there is an urgent imperative to develop new agents. Orally
83 bioavailable agents are particularly important given the predominance of this disease in resource
84 constrained settings.

85 During the process of screening a compound library against fungal pathogens, it was
86 noted by us (M.T. & I.C.) that flubendazole has potent in vitro activity against *Cryptococcus*
87 *neoformans*. A literature search revealed other members of the benzimidazole class (e.g.
88 albendazole and mebendazole) of anti-parasitic agents had previously been demonstrated to
89 have potent in vitro activity against *Cryptococcus neoformans* with minimum inhibitory
90 concentrations (MICs) of 0.16-0.45 mg/L (12, 13). The pharmacological target of the
91 benzimidazoles against *Cryptococcus neoformans* is ß-tubulin (14). The antifungal activity of
92 parenterally administered flubendazole in a murine model of cryptococcal meningitis was

Accepted Manuscript Posted Online

Antimicrobial Agents and Chemotherapy

AAC

Antimicrobial Agents and Chemotherapy

Downloaded from http://aac.asm.org/ on January 15, 2018 by guest

93 confirmed by us in a series of preliminary experiments. Concurrently, we became aware of the
94 efforts by Janssen Pharmaceutica to develop a new orally bioavailable formulation of
95 flubendazole that may be active against filariasis and onchocerciasis. The potential value of this
96 new formulation as an oral medicine for the treatment of cryptococcal meningitis in resource
97 poor healthcare settings was therefore evident.

98 Herein, we describe the *in vitro* activity, putative structure-activity relationships, and the
99 *in vivo* pharmacokinetic-pharmacodynamic relationships of flubendazole against *Cryptococcus*
100 *neoformans*. A hollow fiber infection model of cryptococcal meningitis was developed as a first
101 step for exploring dose-exposure-response relationships. Subsequently, two extensively used
102 and well-characterized laboratory animal models of cryptococcal meningitis were used to
103 provide the experimental foundation for the potential use of oral formulations of flubendazole
104 or its congeners for the treatment of a neglected infection of global significance.

105

Accepted Manuscript Posted Online

Antimicrobial Agents and Chemotherapy

AAC

Antimicrobial Agents and Chemotherapy

Downloaded from http://aac.asm.org/ on January 15, 2018 by guest

106 RESULTS

107 *In vitro studies*

108 Flubendazole displayed potent *in vitro* activity (MIC 0.06-0.25 mg/L; Table 1) against *C.*
109 *neoformans*. The MICs were comparable when EUCAST and CLSI methodology was used.

110 The flubendazole IC_{50} against porcine tubulin was 2.38 µM. Other known tubulin
111 inhibitors display similar efficacy in this assay (e.g. colchicine IC_{50} = 1.15 µM (unpublished data),
112 paclitaxel IC_{50} = 3.9 µM (15) and vinblastine IC_{50} = 5.3 µM (15). These data are consistent with
113 the known mechanism of action of flubendazole.

114 *In vitro DMPK* assessment of commercially available flubendazole powder confirmed a
115 favorable logD7.4 of 2.9. Plasma protein binding was 90.6% and there was low metabolic
116 turnover (Hu Mic Clint = 44 µl/min/mg and Rat Hep Clint = 39 µl/min/10^6 cells). However,
117 aqueous solubility was poor (0.8 µM), which is characteristic of the benzimidazoles. This *in vitro*
118 DMPK assessment was consistent with subsequent *in vivo* observations (see below). Poor
119 aqueous solubility limits absorption through the gut, but once in the bloodstream the drug has
120 favorable pharmacokinetic properties (e.g. ability to pass through cell membranes, low
121 metabolism, and high concentrations of free drug) that enable it to reach the effect site.

122

123 *Docking Studies*

124 There were two principal non-covalent binding interactions between flubendazole and
125 the homology model of *C. neoformans* ß-tubulin. First, the hydroxyl group of Serine 350 acts as a
126 hydrogen bond donor and binds the ketone oxygen of flubendazole (Figure 1A). Second,

Accepted Manuscript Posted Online

Antimicrobial Agents and Chemotherapy

AAC

Antimicrobial Agents and Chemotherapy

Downloaded from http://aac.asm.org/ on January 15, 2018 by guest

127 asparagine (Asn) 247 acted as a hydrogen bond donor via the primary amide with the ketone of
128 the carbamate on flubendazole, but also acted as a hydrogen bond acceptor through the primary
129 carbonyl group of Asn247 and the N-H on the benzimidazole core. There were also several
130 hydrophobic interactions deeper in the binding pocket that involved the benzene ring and the
131 fluorine of flubendazole.

132 Docking studies of flubendazole and human ß-tubulin (Fig 1B) showed that both the N-H
133 of the benzimidazole core and the N-H of the carbamate are hydrogen bond donors (Figure 1B)
134 to the primary amide of the side chain of Asn247. As for the *C. neoformans* interaction, there
135 were hydrophobic interactions present from the para-substituted benzene and the hydrophobic
136 binding pocket. There was a lack of a hydrogen bond acceptor role from the ketone oxygen. This
137 is due to the replacement of Ser350 from the *C. neoformans* active site with Lys350 in humans.
138

139 *Hollow Fiber Infection Model of Cryptococcal Meningoencephalitis*

140 Rapid fungicidal activity was observed in the hollow fiber infection models. Controls
141 grew from an initial density of approximately $\log_{10}$CFU/mL 6 to $\log_{10}$CFU/mL 8-9. Following the
142 administration of flubendazole there was a progressive decline in the fungal density in the
143 hollow fibre in all arms. There was an exposure-dependent decline in fungal burden.
144

145 *Preliminary Studies to Demonstrate In vivo Efficacy of Flubendazole*

146 There was no demonstrable antifungal effect of orally administered flubendazole as pure
147 compound when formulated with sterile distilled water, 0.05% polysorbate 80 in PBS, 5% DMSO,

Accepted Manuscript Posted Online

Antimicrobial Agents and Chemotherapy

AAC

Antimicrobial Agents and Chemotherapy

Downloaded from http://aac.asm.org/ on January 15, 2018 by guest

148 10% PEG400 or 85% hydroxyl-propyl-ß-cyclodextrin (data not shown). Antifungal activity could
149 only be established when pure flubendazole formulated with polysorbate 80 (Tween 80) and
150 injected s.c. to form a depot. Presumably, formulation with polysorbate 80 solubilized
151 flubendazole to an extent that enabled it to become systemically bioavailable. However, this
152 was only observed when flubendazole was administered s.c. This parenteral regimen resulted in
153 a modest reduction in fungal burden of 1-2 $\log_{10}$CFU/g compared with vehicle-treated controls
154 (data not shown). A limited PK study with concentrations measured at a single time-point the
155 end of the experiment also confirmed flubendazole concentrations were quantifiable in plasma
156 and the cerebrum of mice (data not shown).

157 These preliminary pharmacokinetic and pharmacodynamic data provided the impetus for
158 further detailed experiments examining the pharmacodynamics of a new orally bioavailable solid
159 drug nano-dispersion against *Cryptococcus neoformans* developed by Janssen.

160

161 *Pharmacokinetic and Pharmacodynamic Studies of the Flubendazole Nanoformulation in Mice*

162 When flubendazole was formulated as a solid drug nano-dispersion, it was rapidly
163 absorbed after oral dosing and plasma concentrations were readily quantifiable at the first
164 sampling point (i.e. 0.5 hrs. post dose; Figure 3). The pharmacokinetics were linear, with bi-
165 exponential clearance from the bloodstream with a mean and median value of 0.039 and 0.026
166 L/h, respectively (Figure 3). The pharmacokinetic parameters are summarized in Table 2. There
167 was rapid and extensive distribution of drug to the cerebrum of mice and concentrations of

Accepted Manuscript Posted Online

Antimicrobial Agents and Chemotherapy

AAC

Antimicrobial Agents and Chemotherapy

Downloaded from http://aac.asm.org/ on January 15, 2018 by guest

168 flubendazole were consistently higher than those observed in plasma. The AUCserum:
169 AUCcerebrum was 1:4.44.

170 Flubendazole had a significant and discernible antifungal effect in mice. Use of the
171 highest dosage in this study (12 mg/kg) resulted in approximately a 2-3 log reduction in fungal
172 burden relative to controls (Figure 4). This regimen was limited by maximum permissible
173 volumes for oral administration for mice (i.e. 20 mL/kg). In a single experiment in which the
174 effect of 6 mg/kg q12h (i.e. 12 mg/kg/day) was compared to 12 mg/kg/day there was no
175 difference in antifungal effect (data not shown). This is preliminary evidence that the AUC is
176 likely to be the dynamically linked index for flubendazole against *Cryptococcus neoformans*.

177

178 *Pharmacokinetic and Pharmacodynamic Studies in Rabbits*

179 The PK in rabbits was linear with a similar concentration-time profile to that observed in
180 mice. The plasma concentration-time profiles in rabbits had a similar shape to those of mice, but
181 were lower for the dosages used in this study. Despite readily quantifiable plasma
182 concentrations, there was no quantifiable drug concentrations in either the CSF or the cerebrum
183 of rabbits at the time of sacrifice.

184 There was no demonstrable antifungal effect in rabbits receiving 6 mg/kg/day. There
185 may be some effect in rabbits receiving 22.5 mg/kg q24h, but if present the effect was small and
186 these assessments were limited by few animals. There were no statistically significant
187 differences in the area under the $\log_{10}$CFU/g-time curve for each regimen even though this may
188 be a relatively insensitive test of antifungal effect. Furthermore, there was no difference in the

Accepted Manuscript Posted Online

Antimicrobial Agents and Chemotherapy

AAC

Antimicrobial Agents and Chemotherapy

Downloaded from http://aac.asm.org/ on January 15, 2018 by guest

189 fungal burden in the cerebrum at the end of the experiment for any of the groups of rabbits

190 used in this study.

191

Accepted Manuscript Posted Online

Antimicrobial Agents and Chemotherapy

AAC

Antimicrobial Agents and Chemotherapy

Downloaded from http://aac.asm.org/ on January 15, 2018 by guest

192

193 DISCUSSION

194 When given subcutaneously, flubendazole has striking activity in laboratory animal
195 models of filarial diseases such as onchocerciasis and lymphatic filariasis (16). Janssen developed
196 a novel amorphous solid drug nanodispersion to provide a potential new therapeutic option for
197 patients with these neglected tropical diseases. The systemic drug exposure that was enabled by
198 the new formulation mandated GLP toxicology studies before progression to early phase clinical
199 studies. It was already known that flubendazole is clastogenic (i.e. induces chromosomal
200 breakages) and aneugenic (i.e. induces aneuploidy), as well as embryotoxic (17). GLP toxicology
201 studies were performed by Janssen in the rat (5, 15 and 30 mg/kg/day in male rats and 2.5, 5 and
202 10 mg/kg/day in female rats) and in the dog (20, 40 and 100 mg/kg/day) for 2 weeks. These
203 experiments showed evidence of toxicity related to the pharmacological activity of flubendazole
204 in the gastrointestinal tract, lymphoid system and the bone marrow, as well as testicular toxicity
205 in both rat and dog. In the dog, liver toxicity was also observed. As a result, the development
206 program was stopped based on an unacceptable risk/benefit profile in humans. This also halted
207 our own efforts to develop flubendazole for cryptococcal meningitis.

208 Flubendazole has striking *in vitro* activity against *Cryptococcus neoformans* that was
209 evident in the MIC testing and the pharmacodynamic studies in the hollow fiber infection model.
210 There was modest antifungal activity in the murine model, which is not as prominent as that
211 previously described by us for fluconazole, amphotericin B deoxycholate or liposomal
212 amphotericin B (8, 18, 19). There was no unequivocal antifungal activity in the rabbit model of
213 cryptococcal meningoencephalitis, which is largely explained by the absence of detectable

Accepted Manuscript Posted Online

Antimicrobial Agents and Chemotherapy

AAC

Antimicrobial Agents and Chemotherapy

Downloaded from http://aac.asm.org/ on January 15, 2018 by guest

214 flubendazole concentrations in the cerebrum or CSF (despite readily quantifiable plasma
215 concentrations). The in vitro susceptibility testing and data from the hollow fiber model suggests
216 that flubendazole is highly potent and fungicidal if able to reach its fungal target in sufficient
217 concentrations. The diminished activity in the mouse (relative to historical controls) and absence
218 of effect in the rabbit (with non-quantifiable concentrations in the cerebrum and CSF) further
219 support this conclusion. Hence, successful exploitation of the benzimidazole backbone requires
220 careful attention to physiochemical properties that promote absorption across the gut and the
221 ability to partition into sub-compartments of the CNS.

222 Flubendazole did not display a comparable degree of *in vivo* activity to other first-line
223 agents for cryptococcal meningitis (i.e. fluconazole and amphotericin B formulations). Even if
224 the safety profile was not problematic, there is insufficient *prima facie* evidence from either the
225 murine or rabbit models to further study flubendazole as monotherapy for induction therapy in
226 phase II clinical studies. Nevertheless, additional approaches such as the combination with other
227 antifungal agents for induction therapy and/or used as longer-term consolidation and
228 maintenance therapy may have been possible.

229 The potential of derivatives of flubendazole to be useful human medicines depends on
230 the differential activity between cryptococcal and human proteins. Characterization of the β-
231 tubulin genes of *C. neoformans* has been undertaken and two *C. neoformans* β-tubulin genes
232 (*TUB1* and *TUB2*) have been identified. *TUB1* was identified as the primary target of the
233 benzimidazole class of compounds through gene characterization and expression (14). There is
234 90% homology between fungal *TUB1* and human β-tubulin, although the former has not been
235 crystallized and this has prevented definitive structure-activity-relationship docking studies. The

Accepted Manuscript Posted Online

Antimicrobial Agents and Chemotherapy

AAC

Antimicrobial Agents and Chemotherapy

Downloaded from http://aac.asm.org/ on January 15, 2018 by guest

236 ability to develop new agents based on a benzimidazole scaffold or to further exploit β-tubulin as
237 a pharmacological target will depend on the degree of differential activity of a benzimidazole
238 with these proteins. The differential binding identified through the docking and homology
239 modelling of both human β-tubulin (20) and *C. neoformans* var. *grubii* serotype A (strain H99) β-
240 tubulin (14) to the Bos Taurus 1SA0 β-tubulin crystal structure implies an increased number of
241 binding interactions with *C. neoformans* β-tubulin. This may provide the potential to exploit this
242 differential binding to establish a favorable therapeutic index. It is also worth emphasizing that
243 the benzimidazoles may have additional targets beyond β-tubulin that have the further potential
244 to provide differential activity between human and fungal proteins, but this requires further
245 investigation (21–24).

246 The potential utility of congeners of flubendazole now rests with medicinal chemistry
247 programs. Compounds must be synthesized that exhibit differential activity against cryptococcal
248 and human tubulin (if that is possible) so that there is an acceptable safety margin and toxicity
249 profile. Furthermore, the compound must be able to traverse the gut (compounds that are not
250 orally bioavailable will be less clinically valuable) and then the blood-brain-barrier to achieve
251 concentrations that are ideally fungicidal. The latter will be promoted by new molecules that
252 low molecular weight lipophilic compounds that are not substrates for active pumps such as P-
253 glycoprotein. This will undoubtedly also require the use of novel formulation technologies to
254 ensure compounds that are poorly soluble to become useful agents for disseminated infections.

255

Accepted Manuscript Posted Online

Antimicrobial Agents and Chemotherapy

AAC

Antimicrobial Agents and Chemotherapy

Downloaded from http://aac.asm.org/ on January 15, 2018 by guest

256 METHODS

257 *Drug*

258 Flubendazole that was used for determination of MICs, hollow fibre experiments and
259 preliminary murine experiments was purchased from Sigma. Subsequently, definitive
260 pharmacokinetic-pharmacodynamic experiments that were performed with orally administered
261 flubendazole used a solid drug nano-dispersion formulation of flubendazole developed by
262 Janssen Pharmaceuticals (batch BREC-1113-070, Janssen Pharmaceuticals). The stability of this
263 formulation in liquid and solid phases was confirmed for 1 and 6 months, respectively.

264 A 10 mg/mL methylcellulose 4000cps stock solution (100 mL batch) was prepared from a
265 dispersion of 1 g methylcellulose 4000cps with stirring into 70 mL demineralized water heated to
266 70°C-80°C. The solution was stirred for at least 15 minutes followed by the addition of 20 mL of
267 demineralized water. The mixture was stirred until it reached room temperature and was then
268 made up to 100 mL with demineralized water. A total of 50mL of 6 mg/mL spray dried powder
269 suspension was then prepared (this corresponds with 0.6 mg/mL of flubendazole as the active
270 dose in 0.5% methylcellulose). A total of 24.70 g of demineralized water was added to a 50-mL
271 clear glass vial. A total of 0.30 g of spray dried drug was added to the vial which was then closed
272 with a stopper. The vial was vortexed and then homogenized using a polytron disperser. A 25-
273 mL stock solution of methylcellulose 4000cps was added and the vial was vortexed. The
274 suspension was refrigerated at 5°C until dosing for a maximum of 14 days. Prior to dosing the
275 suspension was vortexed.

Accepted Manuscript Posted Online

Antimicrobial Agents and Chemotherapy

AAC

Antimicrobial Agents and Chemotherapy

Downloaded from http://aac.asm.org/ on January 15, 2018 by guest

276 *Strains*

277 The initial *in vitro* susceptibility testing was performed with H99 (ATCC 208821). An
278 additional 49 clinical isolates were obtained from the National Centre for Microbiology Instituto
279 de Salud Carlos III, Madrid, Spain (courtesy Ana Alastruey-Izquierdo and Manual Cuenca-Estrella).
280 These isolates were identified to species level using standard microbiological techniques.

281 *Minimum Inhibitory Concentrations*

282 The minimum inhibitory concentration of flubendazole against H99 (ATCC 208821) and
283 the 49 isolates was estimated using methodology of the European Committee on Antimicrobial
284 Susceptibility Testing (EUCAST; (25)) and Clinical Sciences Laboratory Institute (CLSI; (26)). The
285 endpoint for MIC determination using EUCAST and CLSI was 50% for both methods. MICs were
286 performed in triplicate.

287 *Porcine Tubulin Polymerization Assay*

288 Porcine tubulin is generally used as a surrogate for human tubulin because of its high
289 degree of homology (95%) (27). In the studies described herein, this assay was used to
290 determine the extent of interaction between flubendazole and its putative target as also occurs
291 for assessment of the binding of antineoplastic agents (28, 29). The commercially available
292 porcine tubulin assay (BK011P, Cytoskeleton, Inc. Denver, USA) quantifies the time-dependent
293 polymerization of tubulin to microtubules and thus the ability of tubulin inhibitors to disrupt this
294 process.

295 The porcine tubulin assay was performed according to the manufacturer's instructions.
296 Briefly, the 96-well assay plate was pre-warmed to 37°C prior to use. Five µL of test

Accepted Manuscript Posted Online

Antimicrobial Agents and Chemotherapy

AAC

Antimicrobial Agents and Chemotherapy

Downloaded from http://aac.asm.org/ on January 15, 2018 by guest

297 compound(s) and controls at 0, 1.25, 2.5, 5, 10 µM were aliquoted into each well and pre-
298 warmed for 1 min. Colchicine and DMSO were used as positive and negative controls,
299 respectively. Polymerization was initiated by mixing 45 µL of reaction buffer that contained 2
300 mg/mL of purified porcine brain tubulin, 10 µM fluorescent reporter, PEM buffer (80 mM PIPES,
301 0.5 mM EGTA, 2 mM $MgCl_2$, pH 6.9), 1mM GTP and 20.3% glycerol. Tubulin polymerization was
302 followed by an increase in fluorescence intensity due to the incorporation of a fluorescence
303 reporter into microtubules as polymerization occurred. The change in fluorescence was
304 measured using an excitation and emission wavelength of 360 nm and 450 nm, respectively
305 every 1-min for 1-hr. at 37°C using a Varioskan multimode plate reader (Thermo scientific Inc.).
306 All data points were acquired in triplicate and IC_{50} values were calculated with GraphPad Prism.
307 The IC_{50} value was defined as the drug concentration required to inhibit tubulin polymerization
308 by 50% compared with negative control.

309

310 *Homology Modeling and Docking Studies*

311 While the amino acid sequence of cryptococcal ß-tubulin is known (74% homology with
312 human β-tubulin), the protein has not been crystallized. A homology model was therefore
313 developed to investigate differential binding modes of flubendazole within *C. neoformans* and
314 human β-tubulin. Molecular modelling (Modeller version 9.14, https://salilab.org/modeller/) of
315 both human β-tubulin (20) and *C. neoformans* var. grubii serotype A (strain H99) β-tubulin (14)
316 was undertaken using the Bos Taurus 1SA0 β-tubulin crystal structure (identity: 364/447 (81.4%);
317 similarity: 405/447 (90.6%)).

Accepted Manuscript Posted Online

Antimicrobial Agents and Chemotherapy

AAC

Antimicrobial Agents and Chemotherapy

Downloaded from http://aac.asm.org/ on January 15, 2018 by guest

318 Virtual flubendazole was built in the molecular modelling software Spartan
319 (Wavefunction Inc., Irvine, USA) and energy minimized. Flubendazole was then subjected to a
320 piecewise linear potential (ChemPLP) docking protocol (a scoring function to provide confidence
321 in the docking pose adopted by the molecule), consisting of 10 genetic algorithm (GA) runs
322 before visualization using the molecular visualization system PyMOL with the top scoring
323 compound depicted in Figure 1. The active site binding interactions were selected by identifying
324 those amino acid residues within 4Å of flubendazole when docked into the β- tubulin binding
325 site. Polar contacts between flubendazole and the surrounding amino acids were identified,
326 which aided in the identification of hydrogen bonding interactions that are key in determining
327 the efficacy of a drug against its pharmacological target.

328 Finally, hydrogen bond donor interactions, as well as hydrophobic interactions were
329 identified using the pharmacophore (i.e. an abstract description of molecular features that in this
330 case are necessary for molecular recognition of flubendazole by β-tubulin) search software Zinc
331 Pharmer (https://academic.oup.com/nar/article-lookup/doi/10.1093/nar/gks378) at 4Å for
332 hydrogen bonding interactions and 6Å for hydrophobic interactions.

333

334 *Hollow Fiber Model of Cryptococcal Meningoencephalitis*

335 A new hollow fiber infection model (HFIM) was developed to investigate the *in vitro*
336 pharmacodynamics of flubendazole against *C. neoformans*. The same cartridges (FiberCell
337 Systems, Frederick, MD, USA) and configuration as previously described for bacterial pathogens
338 was used (see for example (30)). The extra-capillary space of each cartridge was inoculated with

Accepted Manuscript Posted Online

Antimicrobial Agents and Chemotherapy

AAC

Antimicrobial Agents and Chemotherapy

Downloaded from http://aac.asm.org/ on January 15, 2018 by guest

339 40 mL of a suspension containing $\log_{10}$CFU/mL 6 of *C. neoformans* var. *grubii* (ATCC 208821;
340 H99). Yeast-extract-peptone-dextrose (YPD) medium was pumped from the central
341 compartment through the cartridge and back again using a peristaltic pump (205 U; Watson-
342 Marlow, United Kingdom). The HFIM was incubated at 37°C in ambient air. The time-course of
343 fungal growth was determined by removing 1 mL from the extra-capillary space of the cartridge
344 and plating serial 10-fold dilutions to YPD agar.

345 The relationship between flubendazole drug exposure and it effect was explored using a
346 range of drug exposures. Since there is no information on the pharmacokinetics of flubendazole
347 in humans, we attempted to produce AUCs that were comparable to those observed in mice.
348 Various dosages of flubendazole were administered q24h by infusion over 1 hour for 8 days to
349 the central compartment using a programmable syringe driver (Aladdin pump; World Precision
350 Instruments, United Kingdom). There was a 24-hour delay in the initiation of flubendazole
351 therapy post inoculation. To generate first-order pharmacokinetics, fresh YPD medium was
352 pumped into the central compartment, and the same volume of drug-containing medium was
353 simultaneously removed and discarded. Positive controls of currently licensed agents were not
354 studied in these experiments.

355

356 *Murine model of cryptococcal meningoencephalitis*

357 A previously described (31) and well-characterized murine model of cryptococcal
358 meningitis was used to investigate the pharmacodynamics of flubendazole. All laboratory animal
359 experiments were performed under UK Home Office project license PPL40/3630 and were

Accepted Manuscript Posted Online

Antimicrobial Agents and Chemotherapy

AAC

Antimicrobial Agents and Chemotherapy

Downloaded from http://aac.asm.org/ on January 15, 2018 by guest

360 approved by the University of Liverpool's Animal Welfare Ethics Review Board. Male CD1 mice
361 were purchased from Charles River and were 20-30 grams at the time of experimentation. An
362 inoculum of 3 x 10^8 CFU in 0.25 mL was used for each mouse. Groups of mice (n=3) were serially
363 sacrificed throughout the experimental period. The brains were removed and homogenized.
364 Serial 10-fold dilutions were plated to YPD agar supplemented with chloramphenicol to
365 enumerate the total fungal burden. Plates were incubated in air at 30°C for at least 48 hours.
366

367 *Pharmacokinetic and Pharmacodynamic Studies of Flubendazole in Mice*

368 Preliminary evidence for the efficacy of flubendazole was obtained by dissolving pure
369 compound in a variety of excipients that included cyclodextrin (F2G, Eccles, UK), DMSO [5%] and
370 polysorbate 80 [10%] and injecting it subcutaneously q24h. Ultimately, only s.c. injection with
371 Tween80 showed any effect. This experiment provided the impetus to further examine the
372 orally bioavailable formulation developed by Janssen (see above).

373 The pharmacokinetics of oral flubendazole was determined with two independently
374 conducted experiments. Treatment was initiated 24 hrs. post-inoculation. Dosages of 2-12
375 mg/kg were used. Only the first dosing interval was studied. A serial sacrifice design was used
376 with groups of n=3 mice that were sacrificed at 0.5, 1, 2, 8 and 24 hrs. post-inoculation.

377 The pharmacodynamics of oral flubendazole was estimated over the course of three
378 separate independently conducted experiments. Groups of n=3 mice were sacrificed at time = 2,
379 24, 48, 96, 144 and 168 hours post inoculation. Dose finding studies were performed using
380 flubendazole 2, 4, 6, 8, and 12 mg/kg q24h orally. The upper dosage was limited by the volume

Accepted Manuscript Posted Online

Antimicrobial Agents and Chemotherapy

AAC

Antimicrobial Agents and Chemotherapy

Downloaded from http://aac.asm.org/ on January 15, 2018 by guest

381 restrictions for mice imposed Home Office project license PPL40/3630. A fourth experiment
382 compared 12 mg/kg q24 with 6 mg/kg q12h to examine whether more fractionated regimens
383 provided any additional antifungal effect.

384 *Rabbit model of cryptococcal meningitis*

385 A previously described and well-characterized rabbit model of cryptococcal
386 meningoencephalitis (32) was used to further investigate the pharmacodynamics of
387 flubendazole. Male New Zealand White rabbits were purchased from Harlan. Rabbits weighed
388 2.5-3 kg at the time of experimentation. Rabbits were immunosuppressed intramuscularly with
389 hydrocortisone 10mg/kg day -1 relative to infection and then daily throughout the experiment.

390 Cryptococcal meningoencephalitis was induced with the intra-cisternal inoculation of
391 0.25 mL of a suspension containing 3.8 x 10^8 CFU/mL under general anesthesia (induced with
392 metedomidine and ketamine). This inoculum results in progressive infection that manifests as an
393 increase in fungal burden in the CSF and reproducible encephalitis. There is minimal clinical
394 disease with no demonstrable neurological signs in the experimental period. Mortality always
395 occurred in the context of cisternal tapping and repeated anesthesia rather than from
396 progressive infection.

397 *Pharmacodynamic and Pharmacokinetic studies in Rabbits*

398 PK-PD relationships in the rabbit were estimated in two independently conducted
399 experiments consisting of 6 rabbits in each experiment. Rabbits were placed under general
400 anesthesia for removal of CSF via intra-cisternal tapping at 48 hour intervals. Over the course of
401 the two experiments there were n=3 controls (1 rabbit died after being tapped), flubendazole 6

Accepted Manuscript Posted Online

Antimicrobial Agents and Chemotherapy

AAC

Antimicrobial Agents and Chemotherapy

Downloaded from http://aac.asm.org/ on January 15, 2018 by guest

402 mg/kg q24h (n=6) and 22.5 mg/kg q24h (n=6). The maximum dosage that was used was limited
403 by the formulation provided by Janssen and the limits of oral gavage in rabbit (15 mL/kg/day).
404 Treatment was initiated 48 hrs. post-inoculation, and continued for 10 days, after which time all
405 rabbits were sacrificed. Thus, the total duration of the experiment was 288 hours.

406

407 *Measurement of flubendazole concentrations using LC/MS/MS*

408 Flubendazole concentrations in all matrices were measured using a validated ultrahigh-
409 performance liquid chromatography tandem mass spectrometry implemented on an Agilent
410 6420 Triple Quad Mass spectrometer and an Agilent 1290 infinity LC system (Agilent
411 Technologies UK Ltd, Cheshire, UK). Flubendazole was extracted by protein precipitation by
412 adding 300 µL of a 50:50 mix of acetonitrile:methanol that contained the internal standard (6,7-
413 Dimethyl-2,3-di(2-pyridyl) quinoxaline; Sigma Aldrich, Dorset, UK) at a final concentration of 1
414 mg/L to 30µL of each matrix.

415 The extraction was performed in 96-well Sirocco protein precipitation plates (Waters,
416 UK). Samples were then shaken for 2 mins and then extracted using a 96-postive pressure
417 manifold (Waters, UK). A total of 200 µL of the supernatant was removed and placed in a 96 well
418 plate. One µL was injected on an Agilent a Zorbax Eclipse Plus C18 column (2.1 by 50 mm, 1.8-m
419 particle size; Agilent Technologies UK Ltd, Cheshire, UK). Chromatographic separation was
420 achieved using a gradient with the starting conditions of a 60:40 mix of A (0.1% formic acid in
421 water) and B (0.1% formic acid in acetonitrile). The ratio of A:B changed to 20:80 over 2 minutes
422 and then returned to the starting conditions (60:40) for 1 minute of equilibration.

Accepted Manuscript Posted Online

Antimicrobial Agents and Chemotherapy

AAC

Antimicrobial Agents and Chemotherapy

Downloaded from http://aac.asm.org/ on January 15, 2018 by guest

The mass spectrometer was operated in multiple reaction monitoring (MRM) scan mode in positive polarity. The precursor ion for flubendazole and internal standard was 314.1m/z, and 313.15 m/z, respectively. The product ion for flubendazole and internal standard was 282.1 m/z and 284.1 m/z, respectively. The source parameters were set as 4000 V for capillary voltage, 350°C for gas temperature, and 60 lb/in^2 for the nebulizer gas.

The standard curve for flubendazole encompassed the concentration range of 0.0005-8.0 mg/L and was constructed using the respective blank matrix. The limit of quantitation was 0.0005 mg/L and the CV% was 12.7% over the concentration range 0.0005-8 mg/L. and the intra and inter-day variation was <12% for all matrices.

Mathematical modeling

The pharmacokinetic and pharmacodynamic datasets from mice were modelled using the program Pmetrics (33) and the following five inhomogeneous differential equations:

Eq. 1 $$XP(1) = B(1) - Ka * X(1)$$

Eq. 2 $$XP(2) = Ka * X(1) - \left(\frac{SCL}{V}\right) * X(2) - Kcp \cdot X(2) + Kpc \cdot X(3) - Kcb \cdot X(2) + Kbc \cdot X(4)$$

Eq. 3 $$XP(3) = Kcp \cdot X(2) - Kpc \cdot X(3)$$

Eq. 4 $$XP(4) = Kcp \cdot X(2) - Kpc \cdot X(4)$$

Eq. 5 $$XP(5) = Kgmax \cdot \left(1 - \left(\frac{\left(\frac{X(4)}{V}\right)^{Hg}}{C50g^{Hg} + \left(\frac{X(4)}{V}\right)^{Hg}}\right)\right) * \left(1 - \left(\frac{X(5)}{popmax}\right)\right) * X(5)$$

Accepted Manuscript Posted Online

Antimicrobial Agents and Chemotherapy

AAC

Antimicrobial Agents and Chemotherapy

Downloaded from http://aac.asm.org/ on January 15, 2018 by guest

441 The system parameters and their units are as follows: *B(1)* (mg) represents the bolus
442 input of flubendazole into the gut. Ka (h^{-1}) is the first order rate constant collecting the gut and
443 the central compartment; SCL (L/h) is the clearance of flubendazole from the central
444 compartment; V (L) is the volume of the central compartment; Kcp (h^{-1}) and Kpc (h^{-1}) are the
445 first-order inter-compartmental rate constants. Kgmax (log_{10}CFU/g/h) and kkillmax
446 (log_{10}CFU/g/h) are the maximal rates of cryptococcal growth and flubendazole-induced kill,
447 respectively. POPMAX (CFU/g) is the maximum theoretical fungal density. C50g (mg/L) and C50k
448 (mg/L) are the concentrations of flubendazole that induce half-maximal effects on growth and
449 kill, respectively. Hg and Hk are the respective slope functions for growth and kill. The initial
450 condition (CFU/g; not shown in the equations) is the fungal density immediately following
451 inoculation, and is estimated along with other parameters.

452 Equations 1, 2, 3 and 4 are pharmacokinetic equations that describe the movement of
453 drug from the gut, throughout the body and into the brain. Equation 1 describes the movement
454 of drug from the gut. Equation 2 describes the rate if change of flubendazole in the central
455 compartment (plasma) with first-order clearance and movement of drug to and from both a
456 peripheral (unmeasured) compartment and the cerebrum. Equations 3 and 4 describe the rate
457 of change of drug in the peripheral and cerebral compartments, respectively. The
458 pharmacodynamics of flubendazole against *Cryptococcus neoformans* is described by Equation 5,
459 which has terms that describe the capacity limited growth of *Cryptococcus*, flubendazole-
460 induced suppression of growth and drug-induced fungal killing. The antifungal activity in the
461 cerebrum is primarily related to concentrations in the cerebrum.

Accepted Manuscript Posted Online

Antimicrobial Agents and Chemotherapy

AAC

Antimicrobial Agents and Chemotherapy

Downloaded from http://aac.asm.org/ on January 15, 2018 by guest

462 A similar model was used to model the PK-PD data from rabbits, but there were some
463 differences. Firstly, no drug was detectable in the brain or the CSF. Therefore, we let plasma
464 concentrations of drug drive the antifungal effect and did not attempt to model the
465 concentration of drug in the central nervous system (as was the case for mice). We directly
466 linked plasma concentrations with the antifungal effect.

467

Accepted Manuscript Posted Online

Antimicrobial Agents and Chemotherapy

AAC

Antimicrobial Agents and Chemotherapy

Downloaded from http://aac.asm.org/ on January 15, 2018 by guest

468 REFERENCES

469 1. Rajasingham R, Smith RM, Park BJ, Jarvis JN, Govender NP, Chiller TM, Denning DW, Loyse
470 A, Boulware DR. 2017. Global burden of disease of HIV-associated cryptococcal meningitis:
471 An updated analysis. Lancet Infect Dis 3099:1–9.

472 2. Jarvis JN, Bicanic T, Loyse A, Namarika D, Jackson A, Nussbaum JC, Longley N, Muzoora C,
473 Phulusa J, Taseera K, Kanyembe C, Wilson D, Hosseinipour MC, Brouwer AE,
474 Limmathurotsakul D, White N, Van Der Horst C, Wood R, Meintjes G, Bradley J, Jaffar S,
475 Harrison T. 2014. Determinants of mortality in a combined cohort of 501 patients with
476 HIV-associated cryptococcal meningitis: Implications for improving outcomes. Clin Infect
477 Dis 58:736–745.

478 3. Denning DW, Hope WW. 2010. Therapy for fungal diseases: Opportunities and priorities.
479 Trends Microbiol 18.

480 4. Perfect JR, Dismukes WE, Dromer F, Goldman DL, Graybill JR, Hamill RJ, Harrison TS, Larsen
481 RA, Lortholary O, Nguyen MH, Pappas PG, Powderly WG, Singh N, Sobel JD, Sorrell TC. 2010.
482 Clinical practice guidelines for the management of cryptococcal disease: 2010 update by
483 the infectious diseases society of america. Clin Infect Dis 50:291–322.

484 5. Bicanic T, Bottomley C, Loyse A, Brouwer AE, Muzoora C, Taseera K, Jackson A, Phulusa J,
485 Hosseinipour MC, Van Der Horst C, Limmathurotsakul D, White NJ, Wilson D, Wood R,
486 Meintjes G, Harrison TS, Jarvis JN. 2015. Toxicity of amphotericin B deoxycholate-based
487 induction therapy in patients with HIV-associated cryptococcal meningitis. Antimicrob
488 Agents Chemother 59:7224–7231.

Accepted Manuscript Posted Online

Antimicrobial Agents and Chemotherapy

AAC

Antimicrobial Agents and Chemotherapy

Downloaded from http://aac.asm.org/ on January 15, 2018 by guest

489 6. **Stamm AM**, **Diasio RB**, **Dismukes WE**, **Shadomy S**, **Cloud GA**, **Bowles CA**, **Karam GH**, **Espinel-**
490 **Ingroff A**. 1987. Toxicity of amphotericin B plus flucytosine in 194 patients with
491 cryptococcal meningitis. Am J Med **83**:236–242.

492 7. **Milefchik E**, **Leal MA**, **Haubrich R**, **Bozzette S a**, **Tilles JG**, **Leedom JM**, **McCutchan JA**, **Larsen**
493 **R a**. 2008. Fluconazole alone or combined with flucytosine for the treatment of AIDS-
494 associated cryptococcal meningitis. Med Mycol **46**:393–5.

495 8. **Sudan A**, **Livermore J**, **Howard SJ**, **Al-Nakeeb Z**, **Sharp A**, **Goodwin J**, **Gregson L**, **Warn PA**,
496 **Felton TW**, **Perfect JR**, **others**, **Harrison TS**, **Hope WW**. 2013. Pharmacokinetics and
497 pharmacodynamics of fluconazole for cryptococcal meningoencephalitis: implications for
498 antifungal therapy and in vitro susceptibility breakpoints. Antimicrob Agents Chemother
499 **57**:2793–2800.

500 9. **Bicanic T**, **Harrison T**, **Niepieklo A**, **Dyakopu N**, **Meintjes G**. 2006. Symptomatic relapse of
501 HIV-associated cryptococcal meningitis after initial fluconazole monotherapy: the role of
502 fluconazole resistance and immune reconstitution. Clin Infect Dis **43**:1069–1073.

503 10. **Scholer HJ**. 1980. FlucytosineAntifungal Chemotherapy. John Wiley & Sons.

504 11. **Polak A**, **Scholer HJ**, **Wall M**. 1982. Combination therapy of experimental candidiasis,
505 cryptococcosis and aspergillosis in mice. Chemotherapy **28**:461–479.

506 12. **Cruz MC**, **Bartlett MS**, **Edlind TD**. 1994. In vitro susceptibility of the opportunistic fungus
507 Cryptococcus neoformans to anthelmintic benzimidazoles. Antimicrob Agents Chemother
508 **38**:378–380.

Accepted Manuscript Posted Online

Antimicrobial Agents and Chemotherapy

AAC

Antimicrobial Agents and Chemotherapy

Downloaded from http://aac.asm.org/ on January 15, 2018 by guest

509 13. **Joffe LS**, **Schneider R**, **Lopes W**, **Azevedo R**, **Staats CC**, **Kmetzsch L**, **Schrank A**, **Poeta M Del**,
510 **Vainstein MH**, **Rodrigues ML**. 2017. The anti-helminthic compound mebendazole has
511 multiple antifungal effects against Cryptococcus neoformans. Front Microbiol **8**:1–14.

512 14. **Cruz MC**, **Edlind T**. 1997. ß-Tubulin genes and the basis for benzimidazole sensitivity of the
513 opportunistic fungus Cryptococcus neoformans. Microbiology **143**:2003–2008.

514 15. **Gertsch J**, **Meier S**, **Tschopp N**, **Altmann K-H**. 2007. New Tubulin Inhibitors from Plants – A
515 Critical Assessment. Chim Int J Chem **61**:368–372.

516 16. **Mackenzie CD**, **Geary TG**. 2011. Flubendazole: a candidate macrofilaricide for lymphatic
517 filariasis and onchocerciasis field programs. Expert Rev Anti Infect Ther **9**:497–501.

518 17. **Tweats DJ**, **Johnson GE**, **Scandale I**, **Whitwell J**, **Evans DB**. 2016. Genotoxicity of
519 flubendazole and its metabolites in vitro and the impact of a new formulation on in vivo
520 aneugenicity. Mutagenesis **31**:309–321.

521 18. **Livermore J**, **Howard SJ**, **Sharp AD**, **Goodwin J**, **Gregson L**, **Felton T**, **Schwartz JA**, **Walker C**,
522 **Moser B**, **Müller W**, **Harrison TS**, **Perfect JR**, **Hope WW**, **Muller W**. 2013. Efficacy of an
523 abbreviated induction regimen of amphotericin B deoxycholate for cryptococcal
524 meningoencephalitis: 3 days of therapy is equivalent to 14 days. MBio **5**:e00725-13.

525 19. **Lestner J**, **McEntee L**, **Johnson A**, **Livermore J**, **Whalley S**, **Schwartz J**, **Perfect JR**, **Harrison T**,
526 **Hope W**. 2017. Experimental Models of Short Courses of Liposomal Amphotericin B for
527 Induction Therapy for Cryptococcal Meningitis.

528 20. **Ravelli RBG**, **Gigant B**, **Curmi PA**, **Jourdain I**, **Lachkar S**, **Sobel A**, **Knossow M**. 2004. Insight

Accepted Manuscript Posted Online

Antimicrobial Agents and Chemotherapy

AAC

Antimicrobial Agents and Chemotherapy

Downloaded from http://aac.asm.org/ on January 15, 2018 by guest

529 into tubulin regulation from a complex with colchicine and a stathmin-like domain. Nature
530 **428**:198–202.

531 21. **Janupally R**, **Jeankumar VU**, **Bobesh KA**, **Soni V**, **Devi PB**, **Pulla VK**, **Suryadevara P**,
532 **Chennubhotla KS**, **Kulkarni P**, **Yogeeswari P**, **Sriram D**. 2014. Structure-guided design and
533 development of novel benzimidazole class of compounds targeting DNA gyraseB enzyme
534 of Staphylococcus aureus. Bioorganic Med Chem **22**:5970–5987.

535 22. **Kaur G**, **Kaur M**, **Silakari O**. 2014. Benzimidazoles: An Ideal Privileged Drug Scaffold for the
536 Design of Multi-targeted Anti-inflammatory Ligands. Mini-Reviews Med Chem **14**:747–
537 767.

538 23. **Li Y**, **Tan C**, **Gao C**, **Zhang C**, **Luan X**, **Chen X**, **Liu H**, **Chen Y**, **Jiang Y**. 2011. Discovery of
539 benzimidazole derivatives as novel multi-target EGFR, VEGFR-2 and PDGFR kinase
540 inhibitors. Bioorganic Med Chem **19**:4529–4535.

541 24. **Matsumoto Y**, **Kakuda S**, **Koizumi M**, **Mizuno T**, **Muroga Y**, **Kawamura T**, **Takimoto-Kamimura**
542 **M**. 2013. Crystal structure of a complex of human chymase with its benzimidazole derived
543 inhibitor. J Synchrotron Radiat **20**:914–918.

544 25. **Arendrup MC**, **Cuenca-Estrella M**, **Lass-Flörl C**, **Hope W**. 2012. EUCAST technical note on
545 the EUCAST definitive document EDef 7.2: method for the determination of broth dilution
546 minimum inhibitory concentrations of antifungal agents for yeasts EDef 7.2 (EUCAST-
547 AFST). Clin Microbiol Infect **18**:E246--E247.

548 26. **National NC for CLS**. 1997. Reference method for broth dilution antifungal susceptibility

Accepted Manuscript Posted Online

Antimicrobial Agents and Chemotherapy

AAC

Antimicrobial Agents and Chemotherapy

Downloaded from http://aac.asm.org/ on January 15, 2018 by guest

549 testing of yeasts. Approved standard M27-A2. NCCLS, Wayne, PA.

550 27. **Hall JL**, **Dudley L**, **Dobner PR**, **Lewis S a**, **Cowan NJ**. 1983. Identification of two human beta-
551 tubulin isotypes. Mol Cell Biol **3**:854–62.

552 28. **Brunner M**, **Albertini S**, **Würgler FE**. 1991. Effects of 10 known or suspected spindle poisons
553 in the in vitro porcine brain tubulin assembly assay. Mutagenesis **6**:65–70.

554 29. **Owellen RJ**, **Hartke CA**, **Dickerson RM**, **Hains FO**. 1976. Inhibition of Tubulin-Microtubule
555 Polymerization by Drugs of the Vinca Alkaloid Class. Cancer Res **36**:1499–1502.

556 30. **Docobo-Pérez F**, **Drusano GL**, **Johnson A**, **Goodwin J**, **Whalley S**, **Ramos-Martín V**, **Ballestero-**
557 **Tellez M**, **Rodriguez-Martinez JM**, **Conejo MC**, **Van Guilder M**, **Rodríguez-Baño J**, **Pascual A**,
558 **Hope WW**. 2015. Pharmacodynamics of fosfomycin: Insights into clinical use for
559 antimicrobial resistance. Antimicrob Agents Chemother **59**:5602–5610.

560 31. **Sudan A**, **Livermore J**, **Howard SJ**, **Al-Nakeeb Z**, **Sharp A**, **Goodwin J**, **Gregson L**, **Warn PA**,
561 **Felton TW**, **Perfect JR**, **Harrison TS**, **Hope WW**. 2013. Pharmacokinetics and
562 pharmacodynamics of fluconazole for cryptococcal meningoencephalitis: Implications for
563 antifungal therapy and in Vitro susceptibility breakpoints. Antimicrob Agents Chemother
564 **57**.

565 32. **Perfect JR**, **Lang SD**, **Durack DT**. 1980. Chronic cryptococcal meningitis: a new experimental
566 model in rabbits. Am J Pathol **101**:177–194.

567 33. **Neely MN**, **van Guilder MG**, **Yamada WM**, **Schumitzky A**, **Jelliffe RW**. 2012. Accurate
568 detection of outliers and subpopulations with Pmetrics, a nonparametric and parametric

Accepted Manuscript Posted Online

Antimicrobial Agents and Chemotherapy

AAC

Antimicrobial Agents and Chemotherapy

pharmacometric modeling and simulation package for R. Ther Drug Monit **34**:467–76.

Downloaded from http://aac.asm.org/ on January 15, 2018 by guest

Accepted Manuscript Posted Online

Antimicrobial Agents and Chemotherapy

AAC

Antimicrobial Agents and Chemotherapy

Downloaded from http://aac.asm.org/ on January 15, 2018 by guest

573

574 **Table 1.** MIC distributions of flubendazole against *C. neoformans* isolates using CLSI and EUCAST

575 methodologies.

Methodology	Number of strains	Number of isolates with MIC (mg/L) of:				
		0.03	0.06	0.125	0.25	0.5
EUCAST[a]	50	1	19	25	5	0
CLSI[b]	50	2	40	8	0	0

576

577 [a] European Committee for Antimicrobial Susceptibility Testing

578 [b] Clinical Laboratory Sciences Institute

579

580

Accepted Manuscript Posted Online

Antimicrobial Agents and Chemotherapy

AAC

Antimicrobial Agents and Chemotherapy

Downloaded from http://aac.asm.org/ on January 15, 2018 by guest

581

582 Table 2. Parameter Values from the PK-PD model fitted to mice

583

Parameter (Units)	Mean	Median	Standard Deviation
Ka (h^{-1})	11.312	14.895	6.594
SCL/F (L/h)	0.039	0.026	0.031
Vc/F (L)	0.051	0.069	0.033
Kcp (h^{-1})	15.741	15.404	6.806
Kpc (h^{-1})	16.997	16.915	5.962
Kcb (h^{-1})	3.446	0.594	4.709
Kbc (h^{-1})	0.056	0.056	0.030
Kgmax (log_{10}CFU/g/h)	0.107	0.098	0.025
Hg	10.338	5.096	9.782
C_{50}g (L/h)	2.036	1.681	1.517
POPMAX (CFU/g)	982934669.178	427055621.187	2281967059.602
IC (CFU/g)	102.255	116.462	60.966
Vb/F (L)	0.277	0.146	0.335

Accepted Manuscript Posted Online

Antimicrobial Agents and Chemotherapy

AAC

Antimicrobial Agents and Chemotherapy

Downloaded from http://aac.asm.org/ on January 15, 2018 by guest

584 Ka (h^{-1}) is the first order rate constant collecting the gut and the central compartment; SCL/F
585 (L/h) is the apparent clearance of flubendazole from the central compartment; V/F and Vb/F (L)
586 are the apparent volumes of the central compartment and brain, respectively; Kcp (h^{-1}) and Kpc
587 (h^{-1}) are the first-order inter-compartmental rate constants. Kgmax (log_{10}CFU/g/h) and kkillmax
588 (log_{10}CFU/g/h) are the maximal rates of cryptococcal growth and flubendazole-induced kill,
589 respectively. POPMAX (CFU/g) is the maximum theoretical fungal density. C50g (mg/L) and C50k
590 (mg/L) are the concentrations of flubendazole that induce half-maximal effects on growth and
591 kill, respectively. Hg and Hk are the respective slope functions for growth and kill.

592

Accepted Manuscript Posted Online

Antimicrobial Agents and Chemotherapy

AAC

Antimicrobial Agents and Chemotherapy

Downloaded from http://aac.asm.org/ on January 15, 2018 by guest

593

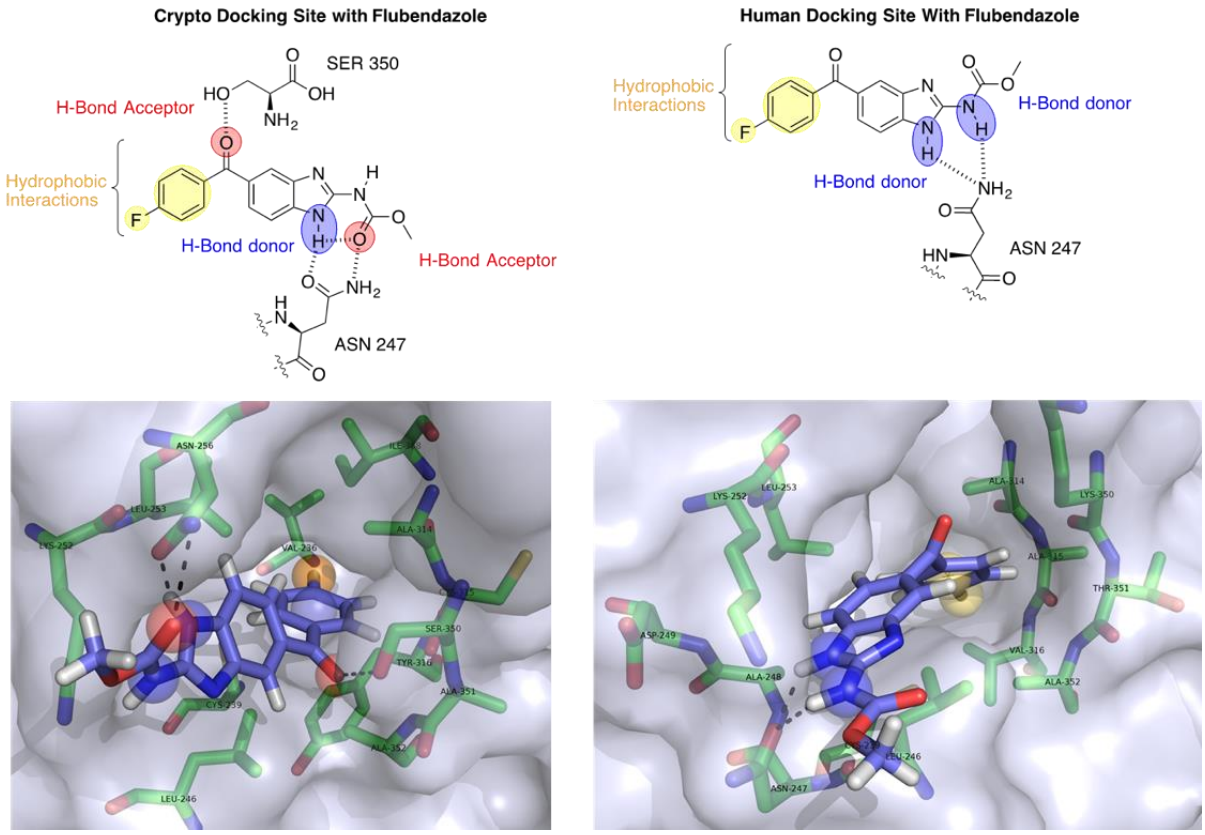

594

595

596 **Figure 1.** Homology model of flubendazole docked with both *C. neoformans* and human β-

597 tubulin. The colours are as follows: red sphere: hydrogen bond donors; blue sphere: hydrogen

598 bond acceptors; yellow sphere: hydrophobic interactions. The docking pose is visualized with

599 PyMOL. Protein is shown as a surface representation coloured 40% transparent light blue.

600 Flubendazole is represented as sticks composed of carbon (light blue); hydrogen (white);

601 nitrogen (dark blue); oxygen (red); and fluorine (cyan). Binding site residues selected around 4 Å

602 are represented as sticks with carbon (green); nitrogen (blue); oxygen (red); and sulfur (yellow).

Accepted Manuscript Posted Online

Antimicrobial Agents and Chemotherapy

AAC

Antimicrobial Agents and Chemotherapy

Downloaded from http://aac.asm.org/ on January 15, 2018 by guest

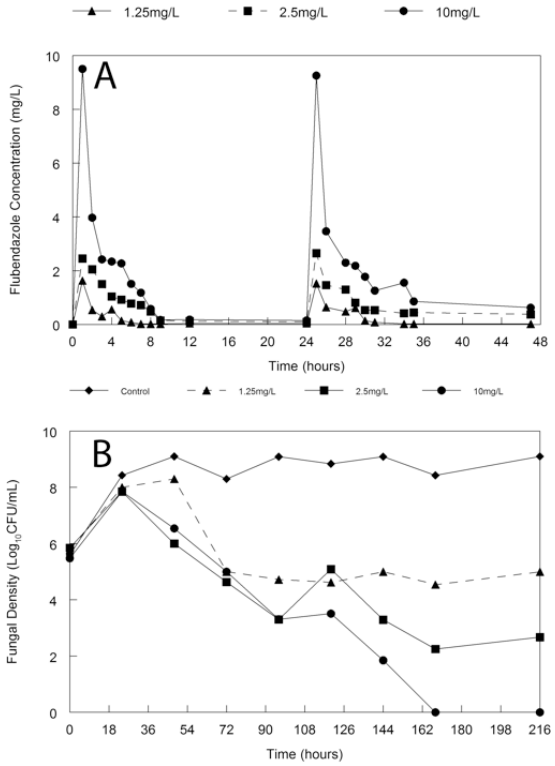

603

604 **Figure 2.** Hollow fiber infection model of cryptococcal meningitis. A, pharmacokinetics of

605 flubendazole with the three arms with intended peak concentrations of 1.25, 2.5 and 10 mg/L;

606 and B, pharmacodynamics in response to flubendazole administered at various dosages q24h.

607 Therapy was initiated 24 hrs. post inoculation after which time *Cryptococcus* had grown from ~6

608 $\log_{10}$CFU/mL to 8 $\log_{10}$CFU/mL.

609

Accepted Manuscript Posted Online

Antimicrobial Agents and Chemotherapy

AAC

Antimicrobial Agents and Chemotherapy

Downloaded from http://aac.asm.org/ on January 15, 2018 by guest

610

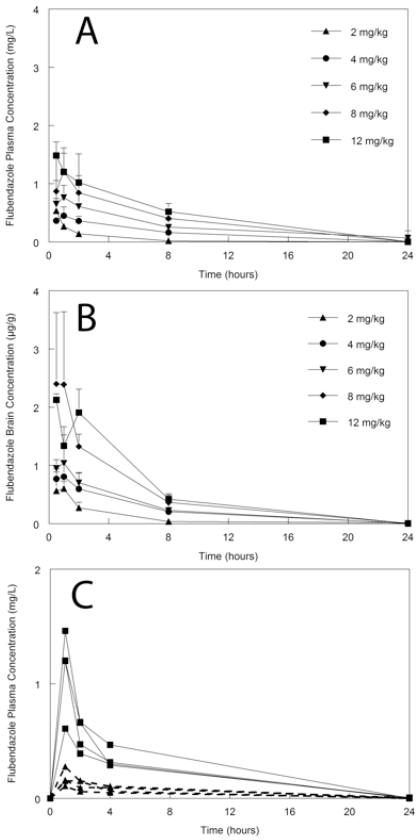

611

612 **Figure 3.** Flubendazole pharmacokinetics in mice and rabbits. A, mouse plasma concentration-

613 time profiles following the administration of flubendazole 2, 4, 6, 8 and 12 mg/kg; B, mouse

614 concentration-time profiles in the brain following the administration of flubendazole 2, 4, 6, 8

615 and 12 mg/kg. Data are mean ± standard deviation of n=3 mice. C, plasma pharmacokinetics in

616 the serum for individual rabbits receiving 6 mg/kg/day (broken lines, solid triangles) and 22.5

617 mg/kg (solid lines, solid squares).

618

Accepted Manuscript Posted Online

Antimicrobial Agents and Chemotherapy

AAC

Antimicrobial Agents and Chemotherapy

Downloaded from http://aac.asm.org/ on January 15, 2018 by guest

619

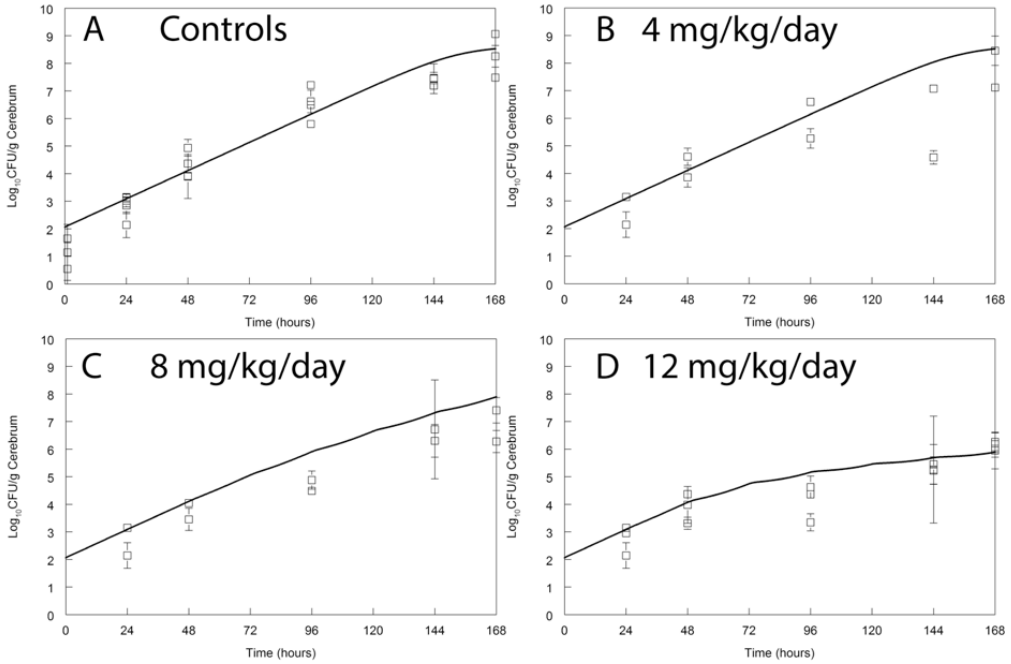

620

621

622 **Figure 4.** Pharmacodynamics of flubendazole in a murine model of cryptococcal meningitis.

623 Flubendazole is administered orally once daily. Data (open squares) are mean ± standard

624 deviation from n=3 mice. The solid line is the fit of the population predicted pharmacokinetic-

625 pharmacodynamic model. The maximally administered dose in this study (12 mg/kg/day)

626 slowed, but did not prevent fungal growth in the brain.

627

Accepted Manuscript Posted Online

Antimicrobial Agents and Chemotherapy

AAC

Antimicrobial Agents and Chemotherapy

Downloaded from http://aac.asm.org/ on January 15, 2018 by guest

628

629

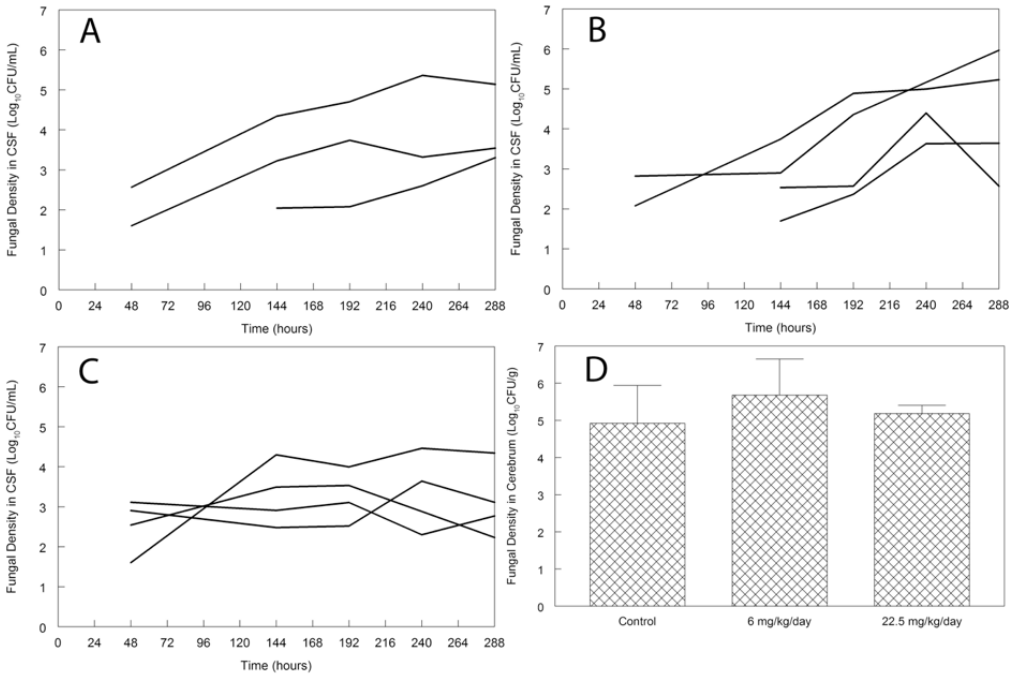

630

631

632 **Figure 5.** Pharmacodynamics of flubendazole in a rabbit model of cryptococcal meningitis. *A,*

633 time-course of fungal burden in the CSF of untreated controls; *B,* time-course of fungal burden in

634 the CSF rabbits treated with flubendazole 6 mg/kg q24h orally; *C,* time-course of fungal burden

635 in the CSF rabbits treated with flubendazole 22.5 mg/kg q24h orally; D, the fungal burden in the

636 cerebrum of rabbits at the end of the experiment (time = 288 hrs. post inoculation and after 10

637 days of treatment with flubendazole). There are no differences in the three groups (p=0.464,

638 ANOVA).

639